A Dynamical Model for the Globular Cluster G1

Baumgardt, H.; Makino, J.; Hut, P.; McMillan, S.L.W.; Portegies Zwart, S.F.

A DYNAMICAL MODEL FOR THE GLOBULAR CLUSTER G1

Holger Baumgardt,[1] Junichiro Makino,[1] Piet Hut,[2]
Steve McMillan,[3] and Simon Portegies Zwart[4]

ABSTRACT

We present a comparison between the observational data on the kinematical structure of G1 in M31, obtained with the *Hubble Space Telescope* Wide Field Planetary Camera 2 and Space Telescope Imaging Spectrograph instruments, and the results of dynamical simulations carried out using the special purpose computer GRAPE-6. We have obtained good fits for models starting from single-cluster King model initial conditions and even better fits when starting our simulations with a dynamically constructed merger product of two star clusters. In the latter case, the results from our simulations are in excellent agreement with the observed profiles of luminosity, velocity dispersion, rotation, and ellipticity. We obtain a mass-to-light ratio of $M/L = 4.0 \pm 0.4$ and a total cluster mass of $M = (8 \pm 1) \times 10^6 \, M_\odot$. Given that our dynamical model can fit all available observational data very well, there seems to be no need to invoke the presence of an intermediate-mass black hole in the center of G1.

Subject headings: black hole physics — globular clusters: individual (G1) — methods: *n*-body simulations — stellar dynamics

1. INTRODUCTION

We report results from a series of *N*-body simulations for the globular cluster G1 in M31. G1 is one of the brightest and most massive globular clusters in the Local Group. Its total luminosity ($M_V = -10.94$ mag) and central velocity dispersion ($\sigma_0 = 25.1 \pm 1.7$ km s^{-1}) are larger than those of any Galactic globular cluster (Meylan et al. 2001; Djorgovski et al. 1997).

Meylan et al. (2001) used virial mass estimates and mass estimates from King-Michie models for G1. They obtained total masses in the range from 7.3×10^6 to $15 \times 10^6 \, M_\odot$ and (for their model 4) a core radius, half-mass radius, and tidal radius of 0.53, 13.2, and 187 pc, respectively. The estimated half-mass relaxation time was 50 Gyr, much longer than the Hubble time.

Gebhardt, Rich, & Ho (2002) have reported evidence for an intermediate-mass black hole of $2.0^{+1.4}_{-0.8} \times 10^4 \, M_\odot$ in the center of G1. Based on velocity profiles obtained with the *Hubble Space Telescope* (*HST*) Space Telescope Imaging Spectrograph (STIS) instrument, they constructed orbit-based axisymmetric models. Varying M/L and the mass of the central black hole, they found a best fit for $M/L = 2.5$ and $M_{BH} = 2 \times 10^4 \, M_\odot$. A model without a central black hole was rejected at a 2σ level.

The presence of such a black hole would be very interesting, for at least two reasons. First, it would lie neatly on the M_{BH}-σ relation for galaxies (Gebhardt et al. 2000; Ferrarese & Merritt 2000). Second, G1 would then be a good example of the type of cluster postulated by Ebisuzaki et al. (2001), some of which may find their way into the center of a galaxy by dynamical friction, where their intermediate-mass black holes may then merge to provide the seeds for supermassive black holes.

However, before embracing such an exciting conclusion it is all the more important to ensure that more conventional explanations of the observational data are ruled out. To this end, we have tried to construct the best possible evolutionary model for G1 as a large globular cluster that is still in the early stages of core collapse, without harboring an intermediate-mass black hole. We have run a set of models with varying initial density profiles, half-mass radii, total masses, and global M/L until we found a model that gave the best fit to the light and velocity profiles of G1.

In § 2, we describe our numerical method. In § 3, we present the results of simulations starting with a single nonrotating cluster, and in § 4 we show what happens when we consider G1 to be the rotating product of a merger of two smaller globular clusters. We briefly summarize in § 5.

2. MODELING METHOD

In order to model the evolution of G1 using *N*-body simulations, we face a scaling and a fitting problem: we can only handle $\sim 10^5$ particles, while G1 contains $\sim 10^7$ stars, and we do not know which values to assign to the initial cluster model parameters such as the total mass and the half-mass radius. We solve the scaling problem by scaling the dynamical parameters in such as way as to reproduce in our model simulations the correct two-body relaxation timescales inferred for G1 from observations. We solve the fitting problem by carrying out a large enough number of runs to allow us to isolate simulations that closely reproduce the observational data. Without the use of the GRAPE-6 computers (J. Makino, T. Fukushige, & K. Namura 2003, in preparation), it would have been unpractical to run the several dozen runs needed to determine our best fits.

We used Aarseth's *N*-body code NBODY4 (Aarseth 1999). All simulated clusters contained $N = 65,536$ stars initially, with a range of masses following the Kroupa (2001) mass function with lower and upper mass limits of 0.1 and 30 $M_\odot$, respectively. Our simulations did not contain primordial binaries, which is a reasonable simplification for a cluster that is still quite far from core collapse. We did not include M31's galactic tidal field, which would have a negligible influence at the position of G1, at least 40 kpc from the center of M31. Since tidal effects are unimportant, we are left with two evolution mechanisms: stellar evolution and two-body relaxation.

Stellar evolution was modeled according to the fitting for-

[1] Department of Astronomy, University of Tokyo, 7-3-1 Hongo, Bunkyo-ku, Tokyo 113-0033, Japan.
[2] Institute for Advanced Study, Einstein Drive, Princeton, NJ 08540.
[3] Department of Physics, Drexel University, Disque Hall, 3141 Chestnut Street, Philadelphia, PA 19104.
[4] Astronomical Institute "Anton Pannekoek" and Section Computational Science, University of Amsterdam, Kruislaan 403, 1098 SH Amsterdam, Netherlands.

mulae of Hurley, Pols, & Tout (2000), using a metallicity of [Fe/H] $= -0.95$, similar to the mean metallicity of G1 as determined by Meylan et al. (2001). We assumed a retention fraction of neutron stars of 15%.

All simulations were carried out for 13 Gyr, and the final density and velocity profiles were obtained from 10 snapshots spanning a 500 Myr period centered at $T = 12$ Gyr. For comparison of our models with the observations of G1, we assume a distance of 770 kpc to M31, so $1''$ corresponds to 3.7 pc. Typically, about 1% of the stars escaped from the cluster during a simulation. Only bound stars were used for the comparison with observations.

We have to scale the parameters of our simulations in order to match the most important stellar evolution and stellar dynamical parameters of the actual G1 cluster. In order to match the relaxation time of G1, we have to increase the radius of our cluster by

$$ r_{h,S} = r_{h,G1} \left(\frac{N_{G1}}{N_S} \right)^{1/3} \left(\frac{\ln \gamma N_S}{\ln \gamma N_{G1}} \right)^{2/3}, \qquad (1) $$

where subscripts G1 and S denote, respectively, the actual values for G1 and those used in our simulations. Effects that strongly depend on the number of particles in the cluster are unimportant before the cluster goes into core collapse, so our models should give a valid description of the dynamical evolution of G1 up to the present time.

In the first set of simulations, we started from isotropic King model conditions with no initial mass segregation and dimensionless central concentrations in the range $4.0 \leq W_0 \leq 11.0$. For each choice of initial density profile, we ran full simulations for a number of choices for the initial physical half-mass radius $r_h(t = 0)$ and mass $M(t = 0)$ of G1 until we could fit the surface density profile of Meylan et al. (2001) over a maximum range in radius while simultaneously obtaining an optimal fit to the observed velocity profile. For the surface density, we scaled our predicted profile by a multiplicative factor to obtain the best fit (in practice changing the M/L predicted by our assumed initial mass function [IMF] by a factor of 1.5–2). For the velocity profile, we used the symmetrized profile shown by Gebhardt et al. (2002) in their Figure 1 and the ground-based value of Djorgovski et al. (1997), who measured a velocity of 25.1 ± 1.7 km s^{-1} inside an aperture of $1''15 \times 7''0$. For each run, a best fit was determined by a χ^2 test against the combined data. With improved estimates for $r_h(t = 0)$ and $M(t = 0)$, a new initial half-mass radius could be calculated and a new simulation was performed. Simulations were performed until the half-mass radius changed by less than 5% between successive iterations. A more detailed description of our simulations and their results will be presented in a forthcoming paper (H. Baumgardt, J. Makino, P. Hut, S. L. W. McMillan, & S. F. Portegies Zwart 2003, in preparation).

3. SINGLE-CLUSTER SIMULATIONS

Figure 1 shows the data for the best fit from among the runs where we started with a single cluster in the form of a King model; here the initial central potential depth was $W_0 = 7.5$. The top panel shows the inferred projected luminosity density. We can see that the fit is very good for $r < 15$ pc. The reason why the model density drops off sharply at large radius is because the initial King model had a tidal radius of 32 pc if we scale it to G1. Two-body relaxation begins to produce an extended halo with a surface density slope ~ -4, but a Hubble
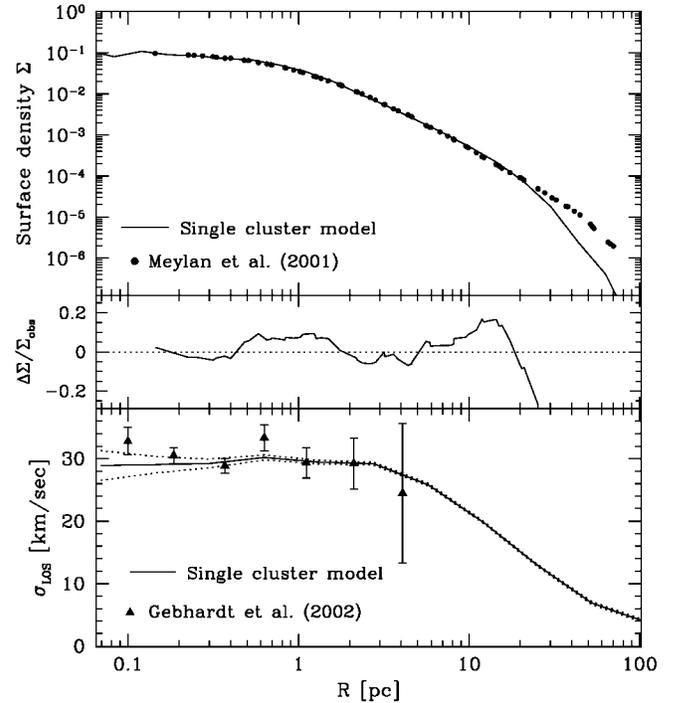

FIG. 1.—Best-fit result, starting from a single $W_0 = 7.5$ King model. *Top*: Surface luminosity profile Σ of the simulations (*solid line*) and the observations (*filled circles*). *Middle*: Values of $\Delta\Sigma/\Sigma_{obs}$, where $\Delta\Sigma = \Sigma_{model} - \Sigma_{obs}$. *Bottom*: Velocity dispersion in the simulations (*solid curve*, with dashed curves indicating the 1 σ error) and observations (*filled triangles with error bars*).

time is too short to let this effect propagate very far into the observed halo. Starting from deeper King models ($W_0 = 8$ or higher) does not solve this problem: such models predict too high a surface density around $r = 10$ pc while still falling short at larger radii. The implication is that G1 must have started with a density distribution more extended than any King model that can be fitted to the bulk of the stars.

The bottom panel shows the velocity dispersion inferred from our $W_0 = 7.5$ model, as compared to the dispersion observed by Gebhardt et al. (2002). For larger W_0-values, our models produce velocities that are too high at the largest observed radii. Models with slightly lower concentration give a somewhat better fit, but when we require the model to reproduce the density as well, the combined requirements clearly point to $W_0 = 7.5$ as producing the best agreement and one that falls within the observational errors everywhere except near the tidal radius artificially imposed by the initial conditions; we address this limitation in § 4.

Note that our model cluster has a mass smaller than those found from multimass King model fits by Meylan et al. (2001). Their extreme values stem from the implicit King model requirement that a cluster has complete mass segregation, which is unphysical in a massive cluster like G1 where the relaxation time is much longer than a Hubble time.

To sum up, an evolutionary model starting from a King model without initial mass segregation reproduces both the luminosity profile and the velocity dispersion profile of G1 rather well. The fits are not perfect, though, on two counts. First, the best-fit model still produces too steep a luminosity profile at larger radii. Second, since we start from a spherically symmetric nonrotating model, in principle we cannot fit the observed rotation profile or ellipticity. The question is whether we can introduce rotation while simultaneously at least pre-
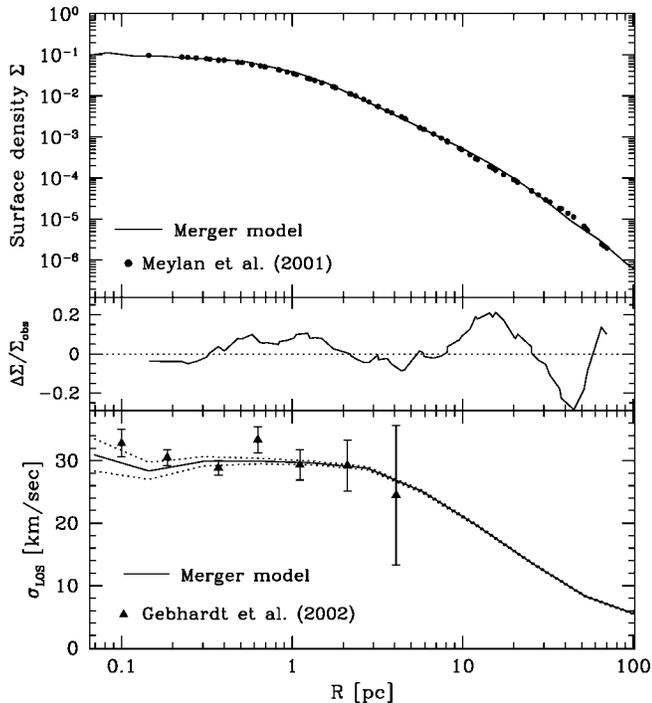
FIG. 2.—Same as Fig. 1, but for the merger model that started from two $W_0 = 6.5$ King models.
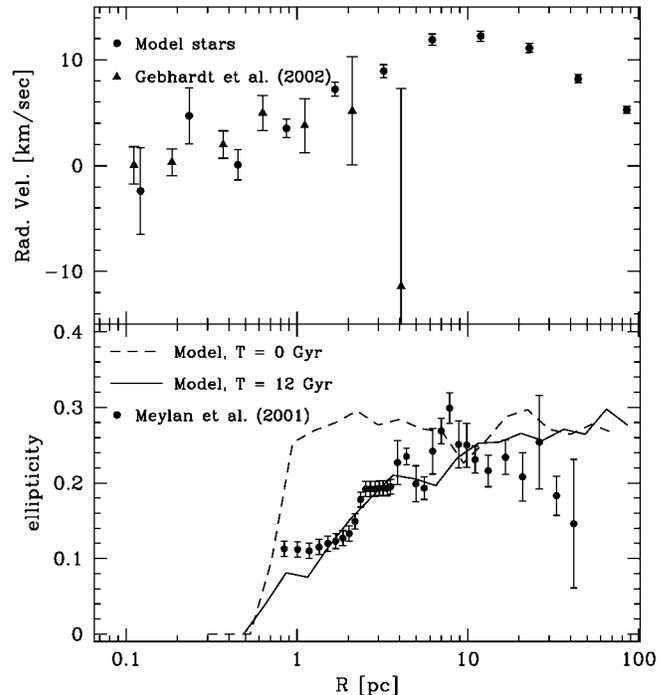

FIG. 3.—Symmetrized radial velocities (*top panel*) and ellipticity profiles (*bottom panel*) for the observations and our best-fit merger model. The ellipticity is defined as $\epsilon = 1 - b/a$, where a and b are the major and minor axis of the best-fit ellipse for the observations and the projected model data. Note that we have omitted the innermost three data points from Meylan et al. (2001), since the ellipticity in the center is not well defined (G. Meylan 2003, private communication).

serving, and hopefully improving, the reasonable fits obtained so far. In § 4, we answer this question affirmatively.

4. MERGER SIMULATIONS

Currently favored scenarios for the formation of star clusters are the collapse of giant molecular clouds or the collision of smaller clouds (Fall & Rees 1985; Fujimoto & Kumai 1997). A collision scenario could easily explain the apparent rotation of G1. It might also account for the run of surface density in the halo, since simulations of the merging of two stellar systems usually give surface density profiles $\Sigma(R) \sim R^{-3.0}$ (Sugimoto & Makino 1989; Makino, Akiyama, & Sugimoto 1990; Okumura, Ebisuzaki, & Makino 1991).

Based on these theoretical hints, we have carried out a series of simulations starting with an early merger of two star clusters. For the sake of simplicity, we have restricted ourselves to the merger of two identical King model clusters on parabolic orbits with initial separation $r_i = 20$ and pericenter separation in N-body units of $p = 1$ (another simulation with $p = 2$ gave similar results). The chosen pericenter distance corresponds to approximately 1.3 half-mass radii for the initial clusters. We used $N = 80,000$ equal-mass stars in our merger simulation without including stellar evolution, a reasonable approximation given that our merger was postulated to occur during formation of the clusters. After the merger product had undergone its violent relaxation, we randomly selected 65,536 stars from among all the stars still bound to the final merger product, assigned masses drawn from the Kroupa (2001) IMF to them, and then started our dynamical evolution simulations for a duration of $T = 13$ Gyr.

Figure 2 shows the final density and velocity dispersion profiles for our best-fit simulations that started with a collision between two $W_0 = 6.5$ initial King models. Note that our simulations now reproduce the observed extended halo very well.

The agreement between the observed and model velocity dispersions is also very good.

Figure 3 compares the rotation and ellipticity profiles of our merger model and the observations. We measured the rotation profile from two directions perpendicular to each other and the minor axis and took the mean of the two directions. The profiles were determined from the radial velocities of all bright stars located in an area between angles of 10° and 40° with respect to the major axis, in order to make an optimal comparison with Gebhardt et al. (2002), who performed their *HST*/STIS spectroscopy at an angle of 25° against the major axis. The agreement between simulated and observed rotation profiles is very good.

Similarly, the ellipticity profile of our merger run is in good agreement with the ellipticity profile of G1 as determined by Meylan et al. (2001; as can be seen in Fig. 3, *bottom panel*). The N-body run starts with a near-constant ellipticity of about $\epsilon = 0.25$. After $T = 12$ Gyr, the cluster core has become almost spherical owing to relaxation effects, while the halo ellipticity has remained unchanged. The observations show a similar drop of ϵ toward the core.

Our success in modeling G1 as a merger product does not necessarily imply that a merger history is the only way to explain its current state. For example, it is also possible that G1 is a heavily stripped remnant of a dwarf spheroidal. What is important is that the observed rotation can be well modeled under at least one set of reasonable assumptions, as we have shown here. The presence of rotation does not invalidate attempts at modeling under the simpler assumption of spherical symmetry; rather, it invites a further fine-tuning of the already good agreement of spherical models.

FORMATION AND EVOLUTION OF G1

TABLE 1
RESULTS OF THE BEST-FITTING N-BODY RUNS

W_0 (1)	Type (2)	r_h (pc) (3)	M ($\times 10^6 \, M_\odot$) (4)	M/L (5)	P_V (6)	$(M/L)_C$ (7)	T_{RH} (Gyr) (8)	$T_R(0)$ (Gyr) (9)
7.5	Single	6.76	7.60 ± 0.76	3.80 ± 0.38	0.20	2.41	30.3	0.292
6.5	Merger	8.21	8.20 ± 0.85	4.10 ± 0.42	0.28	2.44	29.5	0.181

Table 1 summarizes our results for the best-fitting models. It shows W_0 for each initial model, as well as the half-mass radius r_h at $T = 12$ Gyr, and the inferred total mass M and M/L required to give the best-fit velocity dispersions. The half-mass radius shown is the half-mass radius of our models after they were scaled back to G1 by equation (1). The errors given for the values of M and M/L are the statistical errors from the χ^2 fit. The global mass-to-light ratios we obtain in our best fits lie around $M/L \sim 4$, relatively large but still within the range of mass-to-light ratios observed for Galactic globular clusters (Pryor & Meylan 1993). Column (6) gives the probability P_V that our velocity distribution agrees with the observations of Gebhardt et al. (2002) and Djorgovski et al. (1997), determined from a χ^2 test against the combined data.

Columns (7)–(9) of Table 1 give the M/L values inside the core (defined as the region containing the innermost 1% of bright stars) and the half-mass and core relaxation times calculated from the cluster parameters at $T = 12$ Gyr and equation (2-62) of Spitzer (1987). Since the half-mass relaxation time is much longer than a Hubble time, G1 has not yet reached core collapse and the core of G1 is still dominated by low-mass main-sequence stars. Nevertheless, core M/L values are smaller than global ones since mass segregation has caused bright stars, which are more massive than average, to sink into the center. Shortly before core collapse, bright stars will be depleted from the center by the heavier neutron stars and massive white dwarfs, as in the simulations of M15 of Baumgardt et al. (2003).

5. CONCLUSIONS

We have constructed evolutionary models for the massive globular cluster G1. Starting from a $W_0 = 7.5$ King model, we can reproduce both the observed luminosity profile for $r < 15$ pc and the observed velocity dispersion profile. A model starting from the merger of two $W_0 = 6.5$ King models fares even better: it can reproduce the luminosity, velocity dispersion, rotation profiles, and ellipticity for the entire range of observations.

Our simulations were motivated by the recent claim of evidence for a massive central black hole. Given that our dynamical model without a central black hole can fit all available observational data very well, there seems to be no need to invoke the presence of an intermediate-mass black hole. Note that we obtained an excellent fit by varying only the following basic parameters: the central potential W_0, the initial total mass $M(0)$ and total mass-to-light ratio M/L, and the initial half-mass radius $r_h(0)$. Our conclusions are therefore robust and independent of any fine-tuning in initial conditions.

The 2 σ evidence presented by Gebhardt et al. (2002) for a massive black hole is not supported by direct observation of luminosity profile, velocity dispersion, and rotation. It must have come from the data not presented in their paper (e.g., the higher order moments of the velocity profiles together with multiparameter fits to orbit families). Without independent checks or further observational support, we consider the evidence for such a black hole to be inconclusive.

This work is the first example of the successful detailed dynamical modeling of the evolution of a globular cluster with rotation. We have shown how N-body simulations have matured as the most powerful tool to interpret detailed observational data, obviating the need for simplifying assumptions such as spherical symmetry or the use of static (e.g., multimass King) models.

REFERENCES

Aarseth, S. J. 1999, PASP, 111, 1333
Baumgardt, H., Hut, P., Makino, J., McMillan, S. L. W., & Portegies Zwart, S. F. 2003, ApJ, 582, L21
Djorgovski, S. G., et al. 1997, ApJ, 474, L19
Ebisuzaki, T., et al. 2001, ApJ, 562, L19
Fall, S. M., & Rees, M. J. 1985, ApJ, 298, 18
Ferrarese, L., & Merritt, D. 2000, ApJ, 539, L9
Fujimoto, M., & Kumai, Y. 1997, AJ, 113, 249
Gebhardt, K., Rich, R. M., & Ho, L. C. 2002, ApJ, 578, L41
Gebhardt, K., et al. 2000, ApJ, 539, L13
Hurley, J. R., Pols, O. R., & Tout, C. A. 2000, MNRAS, 315, 543

Kroupa, P. 2001, MNRAS, 322, 231
Makino, J., Akiyama, K., & Sugimoto, D. 1990, PASJ, 42, 205
Meylan, G., Sarajedini, A., Jablonka, P., Djorgovski, S. G., Bridges, T., & Rich, R. M. 2001, AJ, 122, 830
Okumura, S. K., Ebisuzaki, T., & Makino, J. 1991, PASJ, 43, 781
Pryor, C., & Meylan, G. 1993, in ASP Conf. Ser. 50, Structure and Dynamics of Globular Clusters, ed. S. Djorgovski & G. Meylan (San Francisco: ASP), 357
Spitzer, L. J. 1987, Dynamical Evolution of Globular Clusters (Princeton: Princeton Univ. Press)
Sugimoto, D., & Makino, J. 1989, PASJ, 41, 1117